Available online at www.sciencedirect.com
ScienceDirect
Journal of Power Sources 160 (2006) 1329–1335
JOURNAL OF POWER SOURCES
www.elsevier.com/locate/jpowsour

Ionic conduction through heterogeneous solids: Delineation of the blocking and space charge effects

B. Kumar*, S. Nellutla, J.S. Thokchom, C. Chen

Metals and Ceramics Division, University of Dayton Research Institute, Dayton, OH 45469-0170, United States

Received 18 January 2006; received in revised form 10 February 2006; accepted 13 February 2006
Available online 31 March 2006

Abstract

The conductivities of an ionic polycrystalline solid lithium iodide (LiI) and covalent, polycrystalline lithium aluminum titanium phosphate (LATP) glass-ceramic material with Al_2O_3 and $Ba_{0.6}Sr_{0.4}TiO_3$ (0.6BST) additions were investigated. It was determined that blocking and space charge effects coexist in these heterogeneous solids. However, their magnitudes differ from one system to another. The most pronounced blocking effect was evident in the LATP–Al_2O_3 system, whereas a dominant space charge effect was observed in the LiI–Al_2O_3 system. The higher dielectric constant of 0.6BST enhanced space charge effect in the LATP–0.6BST system. The space charge effect was also found to be temperature dependent.

Keywords: Glass-ceramic; Composite; Microstructure; Ionic conductivity; Space charge effect

1. Introduction

The phenomenon of ionic conduction in solids is of significant interest, as they are often a choice for components of electrochemical power generators. The energy conversion efficiency, engineering design and deployment limitations of electrochemical power generators greatly depend upon the ionic conductivity of their components. Heterogeneous solids (composites) are used as electrodes in batteries and fuel cells as they provide mixed (electronic and ionic) conductivity and desirable processability on a commercial scale. In spite of this, our understanding of ion transport mechanism in these heterogeneous solids remains tentative, which often leads to speculative approaches for selecting and deploying component materials in these electrochemical power generators.

In heterogeneous solid ionic conductors, an ionic conducting matrix is mixed with a second, insulating phase, thus forming a composite. Prior literature [1–3] has explained the effect of the insulating phase on conductivity in terms of space charge and/or blocking effects. However, at times one effect is invoked arbitrarily over the other to explain and account for conductivity variation in a given heterogeneous system. Furthermore, material parameters of the constituents of a given heterogeneous system that are useful for enhancing the space charge effect are not readily identifiable.

The intent of this paper is to investigate ionic conduction through heterogeneous solids in lithium iodide (LiI)–alumina (Al_2O_3) and lithium aluminum titanium phosphate (LATP) glass-ceramic–Al_2O_3/$Ba_{0.6}Sr_{0.4}TiO_3$ (0.6BST) systems. The LiI–Al_2O_3 system has been of significant interest after Liang [4] reported that the intrinsic conductivity of lithium iodide doped with 35–45 mol% Al_2O_3 was enhanced by orders of magnitude as compared to that of LiI conductivity. The enhancement in conductivity has been explained on the basis of space charge formation at the LiI–Al_2O_3 interface [5]. The LATP–Al_2O_3 and LATP–0.6BST systems are of much recent origin. The high ionic conductivity in the LATP glass-ceramic material was reported by Fu [6]. The LATP glass-ceramic primarily consists of highly conductive $Li_{1+x}Ti_{2-x}Al_x(PO_4)_3$ ($x \sim 0.3$) phase. The highly conductive phase is a derivative of $LiTi_2(PO_4)_3$ which possesses rhombohedral structure (space group $R\bar{3}C$) with an open three-dimensional framework of TiO_6 octohedra sharing all corners with PO_4 tetrahedra. The lithium ion occupies interstitial sites and its conduction takes place along the *c*-axis. The structure of $Li_{1+x}Ti_{2-x}Al_x(PO_4)_3$ implies the existence of Ti–O–P and Al–O–P bonds of covalent nature to form the basic network. The network structure also allows for the presence of conduction channels for fast lithium ion transport.

* Corresponding author. Tel.: +1 937 229 3452; fax: +1 937 229 3433.
E-mail address: kumar@udri.udayton.edu (B. Kumar).

0378-7753/$ – see front matter
doi:10.1016/j.jpowsour.2006.02.062

In the LiI–Al_2O_3 system, the matrix (LiI) is primarily an ionic compound that may ionize at elevated temperatures, thus forming Schottky types of defects. Adsorption of the ionic species on the surface of Al_2O_3 particles can be anticipated. For example, an iodide ion (I^-) can be adsorbed onto the Al_2O_3 surface, making it negatively charged. The charged Al_2O_3 surface must now be balanced by the positively charged region around it. In equilibrium, a double spherical region exists which must be associated by a potential difference. The double layer region can also be characterized as space charge, which is known to augment transport of conducting ions and thus conductivity.

The LATP–Al_2O_3 and LATP–0.6BST systems are conspicuously different as compared to the LiI–Al_2O_3 system. The LATP glass-ceramic host primarily possesses covalent bonding. The high lithium ion conductivity arises from the hopping of lithium ions within crystallographic channels made by the network of Ti–O–P and Al–O–P bonds. The adsorption of ionic species onto the Al_2O_3 and 0.6BST nanoparticle surface is a remote possibility. The space charge effect may not be operative, and one can expect only the blocking effect. Therefore, the conductivity of the LATP–Al_2O_3 and LATP–0.6BST systems should decrease with the gradual addition of Al_2O_3 and 0.6BST.

The choice of Al_2O_3 and 0.6BST was determined on the basis of their dielectric constants. Al_2O_3 is a low dielectric constant (∼10) ceramic, whereas 0.6BST is a ferroelectric ceramic having the Curie temperature around ambient temperature and the material possesses a very high dielectric constant (∼10,000–15,000) at that temperature.

The paper will present, analyze and discuss experimental ionic conductivity data in the LiI–Al_2O_3, LATP–Al_2O_3 and LATP–0.6BST systems with an objective to delineate the blocking and space charge effects. It is hoped that the experimental data and analyses will lead to a better understanding of the two effects and allow processing of heterogeneous systems for enhanced conductivity in an electrochemical power generator.

2. Experimental

2.1. Processing of heterogeneous solids

2.1.1. LiI–Al_2O_3 system

Based on the prior work of Liang in the LiI–Al_2O_3 system [4], a composite of 0.6LiI:0.4Al_2O_3 stoichiometry (reported to provide the highest conductivity) was chosen. The raw materials were as-received LiI (Alfa Aesar) and Al_2O_3 (NanoTek®, particle size < 47 nm). The Al_2O_3 was dried at 600 °C for 24 h in an inert environment and then cooled to room temperature. The dried Al_2O_3 was transferred to a dry box. Small amounts of LiI (2.808 g) and dried Al_2O_3 (1.358 g) were weighed and mixed inside a dry box. The mixed batch was contained inside a dried quartz tube, which was corked before being removed from the dry box. The quartz tube was subsequently sealed using an oxyacetylene torch.

The sealed quartz tube was then heated to 550 °C using an electric furnace and kept at this temperature for 17 h. It was then quenched to room temperature, transferred to the dry box and broken to remove the composite specimen for further characterization.

The 0.6LiI:0.4Al_2O_3 composite (300 mg) was loaded into a die and heated to 100 °C before pressing into a disc of ∼12.68 mm diameter and 1–2 mm thickness with 690 MPa of pressure. The disc was removed from the die after it was cooled to room temperature. After removal, the disc was loaded in the conductivity cell and placed between two stainless steel (SS) electrodes.

2.1.2. LATP–Al_2O_3 and LATP–0.6BST systems

The 30 g batch of $14Li_2O{\cdot}9Al_2O_3{\cdot}38TiO_2{\cdot}39P_2O_5$ (mol%) glass was prepared using reagent grade chemicals Li_2CO_3 (Alfa Aesar), Al_2O_3 (Aldrich, particle size < 10 μm), TiO_2 (Acros Organics) and $NH_4H_2PO_4$ (Acros Organics) as the raw materials. An appropriate amount of these chemicals was properly weighed and mixed together in an agate mortar and pestle for 0.5 h. This mixture was homogeneously mixed for 1 h in a glass jar using a roller mill. Later, the mixed batch was placed in a platinum crucible and melted in an electric furnace. Initially it was heated to 700 °C and kept at this temperature for 1 h to release volatile products. The mixture was then heated up to 1450 °C and melted at this temperature for 1.5 h. This melt was poured onto a preheated (550 °C) SS plate and pressed into a thin plate with another preheated SS plate (250 °C). It was then annealed in air at 550 °C for 2 h and subsequently furnace cooled. The annealed glass was crystallized at 950 °C for 12 h. This crystallization treatment led to the high conductivity LATP glass-ceramic material [7]. The LATP glass-ceramic was powdered into fine particle size of 1–75 μm. This particle size distribution was obtained by screening the hand ground LATP powder. An appropriate amount of LATP powder and Al_2O_3 (NanoTek®, particle size < 47 nm) and 0.6BST (TPL Inc., particle size < 100 nm) was mixed thoroughly in a mortar and pestle inside the dry box. The volume percent of Al_2O_3 and 0.6BST were varied from 2 to 10%. The composite powder mixture (400–500 mg) was pressed with 690 MPa into discs of ∼12.68 mm diameter and 1–2 mm thickness. These samples were sintered at 950 °C for 12 h. These sintered samples were polished using silicon carbide abrasive paper. A 0.5 μm thick gold coating was sputtered on both the sides of the sample to obtain good electrical contact before loading it in the conductivity cell between SS electrodes.

2.2. Electrical conductivity measurement

The electrical conductivity of each specimen was measured by the AC impedance technique in the −41 to 107 °C temperature range. For the AC technique a Solarton 1260 impedance analyzer with 1287 electrochemical interface was used to obtain impedance data in the 0.1–10^6 Hz frequency range.

2.3. Electron microscopy

The microstructure was investigated by means of scanning electron microscopy (SEM, JEOL Model JSM-840). The SEM studies were conducted on a polished and thermally etched surface, and the average grain size was determined by counting the grains and dividing by area.

3. Results and discussion

3.1. Lithium iodide and alumina composite

Fig. 1 shows typical AC impedance spectra of LiI and $0.6LiI:0.4Al_2O_3$ composite specimens. The impedance of LiI is associated with the large semicircle starting from the origin and ending at about $1.6 \times 10^6\ \Omega$ implying that the resistance of the LiI specimen is about $1.6 \times 10^6\ \Omega$. The impedance of the $0.6LiI:0.4\ Al_2O_3$ composite is barely noticeable and confined near the origin. This experimental evidence suggests that the addition of Al_2O_3 reduced the resistance of the composite specimen. The impedance spectrum of the composite specimen is shown by the inset of Fig. 1 on an expanded scale. The semicircle in this case begins at the origin and ends at about $58 \times 10^3\ \Omega$. Comparing the impedance of the two specimens it is noted that the resistance of the composite specimen is reduced by a factor of about 27 at 27 °C due to the addition of Al_2O_3.

Fig. 2 shows the Arrhenius plots of LiI and $0.6LiI:0.4Al_2O_3$ composite specimens obtained at a number of different temperatures in the 27–77 °C temperature range. The conductivity (σ) data fit the Arrhenius equation as expressed by equation:

$$\sigma = A \exp\left(\frac{-E_a}{RT}\right)$$

where A is the pre-exponential factor, E_a the activation energy and R is the gas constant.

The conductivity of the composite specimen increased by nearly two orders of magnitude at all temperatures. The slope of the temperature dependent conductivity data allows one to calculate the activation energy, E_a, which was conducted for both the specimens. The activation energies for LiI and $0.6LiI:0.4Al_2O_3$ were calculated to be 0.51 and 0.57 eV, respectively. The difference in the computed activation energies is insignificant, which suggests that the basic transport mechanism of the lithium in both the specimens remained the same. Liang [4] reported activation energy of 0.43 eV for a similar composition.

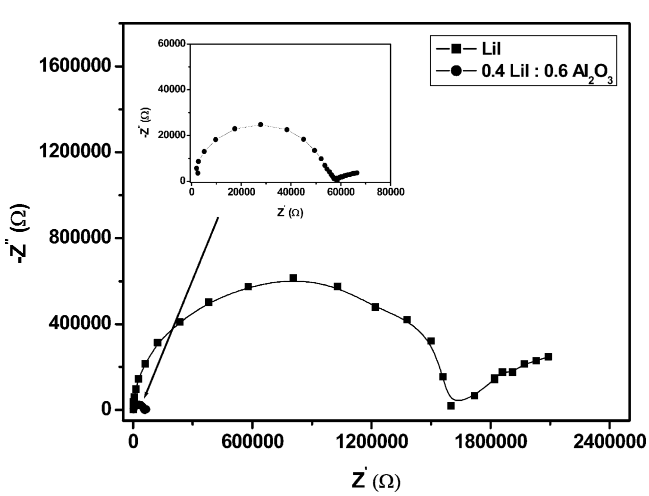

Fig. 1. Typical impedance spectra of LiI and $0.6LiI:0.4Al_2O_3$ composite at 27 °C.

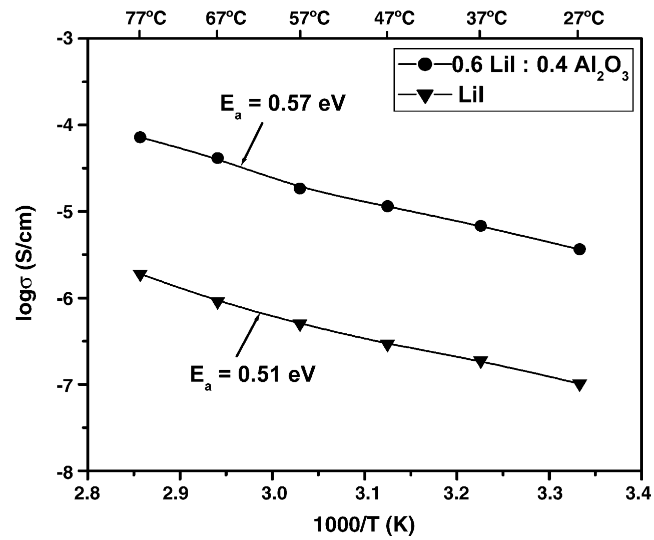

Fig. 2. Arrhenius plots of LiI and $0.6LiI:0.4Al_2O_3$ composite.

To ensure reproducibility of the data, three batches of $0.6LiI:0.4Al_2O_3$ specimens were prepared. The electrical properties of these three specimens as computed from the AC impedance spectra are presented in Fig. 3. There is a slight variation in conductivities among the three batches; nonetheless, they remain much higher than the conductivity of the LiI specimen. The activation energies for the lithium ion transport also vary from 0.54 to 0.69 eV among the three batches.

It should be noted that the reproducibility of the experimental data as presented in Fig. 3 might also have been affected by specimen preparation techniques such as batching, mixing and melting, and the thermal history in addition to the error involved in the impedance measurement. Therefore, the reproducibility of the data in Fig. 3 accounts for all the aforementioned origins of experimental errors. It is also noted that the error in

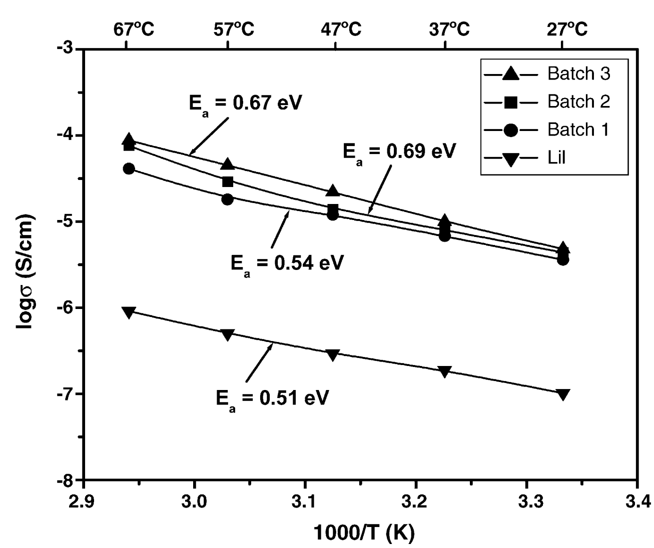

Fig. 3. Reproducibility of conductivity for three $0.6LiI:0.4Al_2O_3$ composite batches and their comparison with LiI.

the reproducibility increases with increasing temperature, which may have some significance. A relatively large variation in the activation energy may have resulted from all these experimental errors.

The effect of volume percent on the conductivity of a composite such as the LiI–Al_2O_3 system is schematically shown in Fig. 4. The proposed trend in conductivity as a function of volume fraction of the inert phase in a heterogeneous solid is based on the analysis of experimental conductivity data on a wide range of material systems. At low volume fractions, the space charge effect is the major contributor. However, as the volume fraction increases beyond a certain point, the blocking effect becomes dominant leading to a precipitous drop in conductivity. A similar trend in the LiI–Al_2O_3 system has been reported by Liang [4] and Maier [1].

3.2. LATP glass-ceramic and its composite with Al_2O_3 and 0.6BST nanoparticles

3.2.1. Microstructure

A scanning electron micrograph of a polished and thermally etched surface of LATP glass-ceramic is shown in Fig. 5. The existence of dense, well-packed, interlocking and random orientation of the crystals is evident in Fig. 5. The average grain size is about 1 μm which is associated with the $Li_{1+x}Ti_{2-x}Al_x(PO_4)_3$ crystalline phase where $x \sim 0.3$. $AlPO_4$ phase is also present in the microstructure, primarily at the grain boundaries. Further information on the crystal chemistry and properties of the LATP glass-ceramic can be found elsewhere [7].

3.2.2. Impedance and conductivity

Fig. 6 shows a typical impedance spectra of LATP and LATP–Al_2O_3 (2 vol%) specimens at 27 °C. The impedance of LATP is depicted by a semicircle starting from the origin and ending at about 3200 Ω. The impedance of the LATP was altered significantly by the introduction of 2 vol% Al_2O_3. The resistance of the specimen as measured by the diameter of the semicircle increased by a factor of 5.

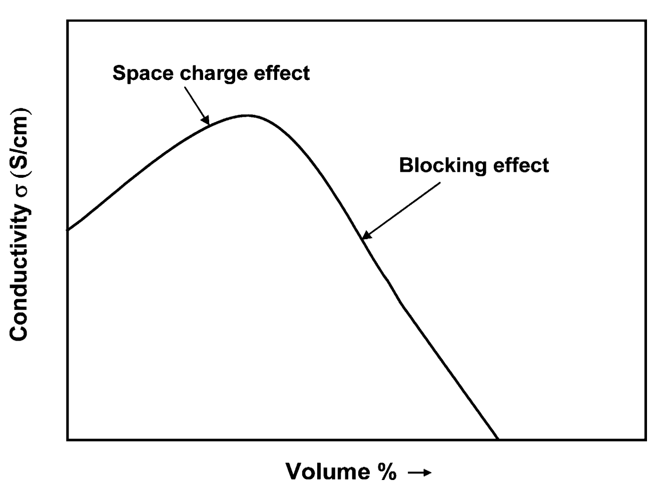

Fig. 4. Schematic presentation of the effects of inert dopant on the conductivity of composites.

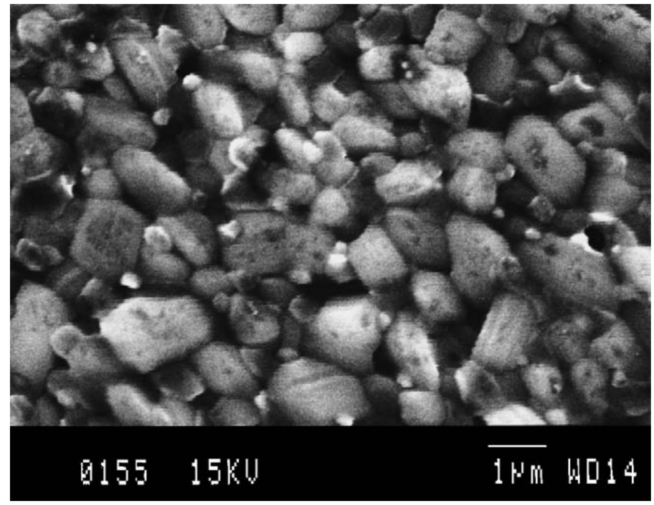

Fig. 5. Microstructures of LATP glass-ceramic of a polished and thermally etched surface.

Fig. 7 depicts Arrhenius plots of LATP and its composite with 2, 5, 10 vol% Al_2O_3. It is evident that the addition of Al_2O_3 in LATP reduces its conductivity. However, the nature of conductivity reduction varies from specimen to specimen. In the case of LATP–2 vol% Al_2O_3 there is a minor inflection in the Arrhenius plot in the 27–47 °C temperature range. The inflection becomes prominent in the case of LATP–5 vol% Al_2O_3 specimen. The inflection has transformed into a peak and the conductivities at −40 and 107 °C were reduced by approximately four and seven orders of magnitude, respectively, in the case of the LATP–10 vol% Al_2O_3 specimen. The drastic reduction in conductivity and occurrence of the peak will be explained later with a physical model.

Barium titanate ($BaTiO_3$) is an important ferroelectric ceramic which displays a very high dielectric constant near the Curie temperature. Barium strontium titanate ($Ba_xSr_{1-x}TiO_3$) is obtained by doping $BaTiO_3$ with SrO, which shifts the ferroelectric transition to lower temperature. In this work, 0.6BST was used because of its much higher dielectric constant

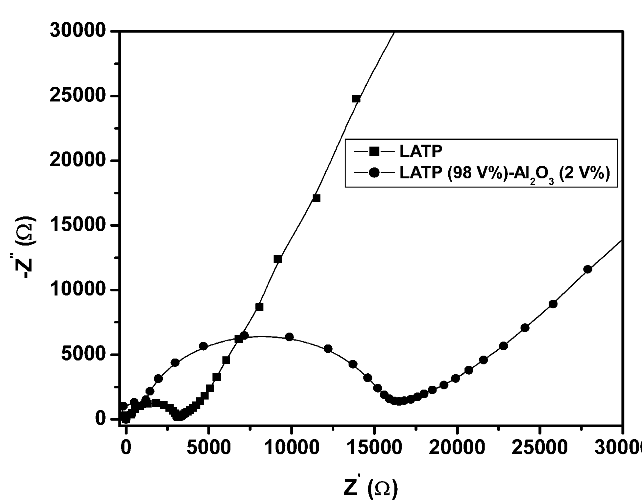

Fig. 6. Typical impedance spectra of LATP and LATP–Al_2O_3 (2 vol%) composite at 27 °C.

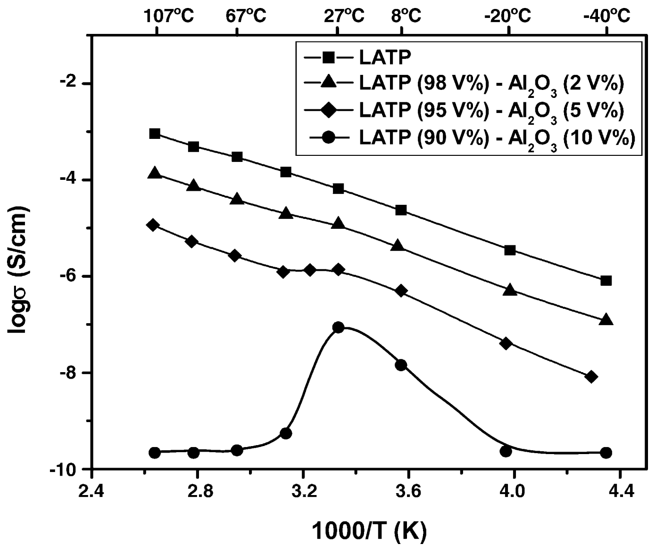

Fig. 7. Arrhenius plots of LATP and its composites with different volume percent of Al_2O_3.

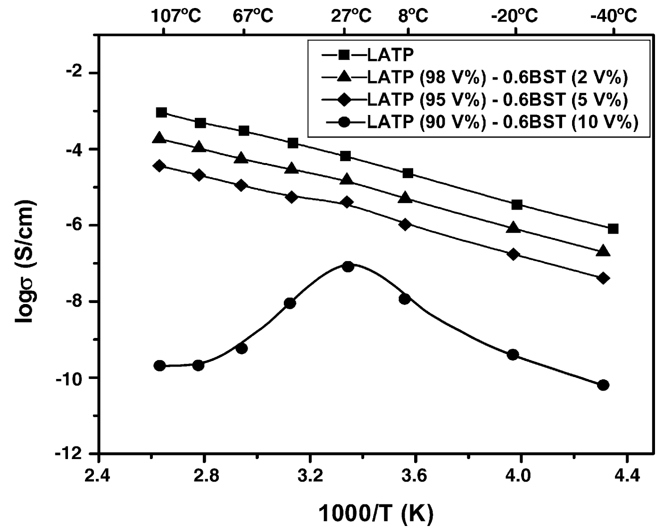

Fig. 8. Arrhenius plots of LATP and its composites with different volume percent of 0.6BST.

(∼10,000–15,000) as compared to Al_2O_3. It was anticipated that the higher dielectric constant 0.6BST would interact differently with LATP and have an effect on the conductivity.

Fig. 8 shows Arrhenius plots of LATP and its composite with 0.6BST. These specimens also exhibit behavior similar to the LATP–Al_2O_3 composites. An inflection around 27 °C for 2 and 5 vol% 0.6BST specimens and a conductivity peak for 10 vol% 0.6BST are evident in Fig. 8.

Fig. 9 shows conductivity data plots of LATP, LATP–Al_2O_3 (2 vol%) and LATP–0.6BST (2 vol%). The addition of both Al_2O_3 and 0.6BST decreased conductivity in the −40 to 107 °C temperature range; however, the effect of Al_2O_3 is more pronounced than the 0.6BST in reducing the conductivity. It is believed that the high dielectric constant of 0.6BST in the temperature range has minimized its blocking effect impact. The detailed experimental data of these specimens are also presented in Table 1.

Fig. 10 presents Arrhenius plots of LATP, LATP–Al_2O_3 (5 vol%) and LATP–0.6BST (5 vol%). Again, in these specimens a trend similar to Fig. 9 is noted. The conductivity data of specimens containing Al_2O_3 and 0.6BST are further depressed as compared to the LATP and both specimens show a clear inflection point around 30 °C. Additional data on these specimens are presented in Table 2. Again, the suppressed blocking effect as evidenced by the high temperature (>27 °C) segment of the conductivity curve of the 0.6BST specimen is attributed to its high dielectric constant.

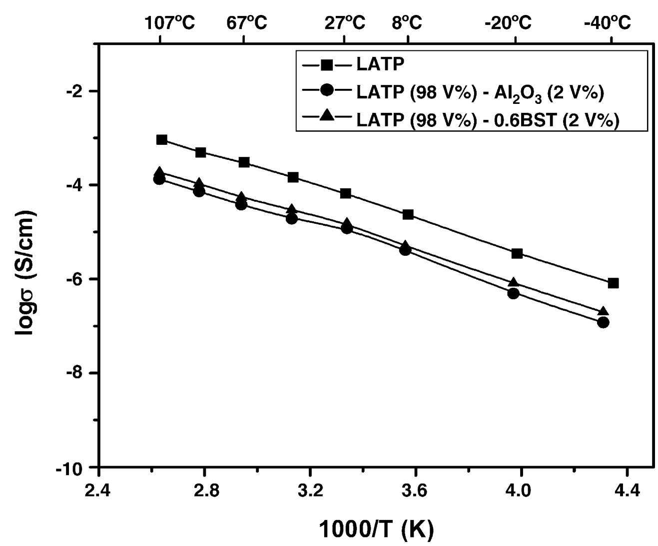

Fig. 9. Arrhenius plots of LATP–Al_2O_3 (2 vol%) and LATP–0.6BST (2 vol%) composites.

Table 1
Resistance and conductivity values of LATP–Al_2O_3 and LATP–0.6BST composites with 2 vol% dopant

Temperature (°C)	1000/*T* (K)	LATP–Al_2O_3			LATP–0.6BST		
		R (Ω)	σ (S cm^{-1})	log σ (S cm^{-1})	*R* (Ω)	σ (S cm^{-1})	log σ (S cm^{-1})
−41	4.31	1.65E+06	1.19E−07	−6.92	1.84E+06	2.00E−07	−6.70
−21	3.97	3.99E+05	4.94E−07	−6.31	4.49E+05	8.21E−07	−6.09
8	3.56	4.73E+04	4.16E−06	−5.38	7.39E+04	4.99E−06	−5.30
26	3.34	1.55E+04	1.27E−05	−4.90	2.43E+04	1.52E−05	−4.82
47	3.13	9.73E+03	2.02E−05	−4.69	1.24E+04	2.98E−05	−4.53
67	2.94	4.56E+03	4.31E−05	−4.37	6.72E+03	5.48E−05	−4.26
87	2.78	2.32E+03	8.47E−05	−4.07	3.49E+03	1.06E−04	−3.97
107	2.63	1.09E+03	1.81E−04	−3.74	1.97E+03	1.87E−04	−3.73

Table 2
Resistance and conductivity values of LATP–Al_2O_3 and LATP–0.6BST composites with 5 vol% dopant

Temperature (°C)	1000/*T* (K)	LATP–Al_2O_3			LATP–0.6BST		
		R (Ω)	σ (S cm^{-1})	log σ (S cm^{-1})	*R* (Ω)	σ (S cm^{-1})	log σ (S cm^{-1})
−41	4.31	2.35E+07	8.37E−09	−8.08	3.30E+06	4.04E−08	−7.39
−21	3.97	4.80E+06	4.10E−08	−7.39	7.67E+05	1.73E−07	−6.76
8	3.56	3.91E+05	5.04E−07	−6.30	1.27E+05	1.05E−06	−5.98
26	3.34	1.42E+05	1.39E−06	−5.86	3.26E+04	4.08E−06	−5.39
47	3.13	1.60E+05	1.23E−06	−5.91	2.41E+04	5.53E−06	−5.26
67	2.94	7.47E+04	2.68E−06	−5.57	1.18E+04	1.13E−05	−4.95
87	2.78	3.91E+04	5.26E−06	−5.28	6.44E+03	2.07E−05	−4.68
107	2.63	1.90E+04	1.15E−05	−4.94	3.71E+03	3.59E−05	−4.44

3.3. Physical models affecting conductivity of composites

There are two physical situations that need to be considered and analyzed to explain conductivity data of composites. These two situations – blocking and space charge models – and have been proposed earlier to explain conductivity of polymer–ceramic and ceramic–ceramic composites [2,3]. The influence of a blocking entity is perhaps easier to visualize and is schematically shown in Fig. 11(a). Charged particles will move forward in the direction of the applied field, E_a. The blocking entity will impede forward motion of conducting ions and they will be scattered to assume another path in the direction of the field. This blocking effect will lead to an increased resistance and hence reduced conductivity. It is also anticipated that the foreign, blocking entity will form an interface with the host matrix. The interfaces are generally electrically active, leading to generation and annihilation of electrons, electron holes and ions. For example, in the case of the LiI–Al_2O_3 system, ionized species such as Li^+ and I^- may interact and form a charged Al_2O_3 surface. It is also known that a charged surface is associated with an electric field. Such an electric field will accelerate transport of conducting ions such as shown in Fig. 11(b).

The difference in dielectric constant between the host LATP and the dopant phase such as Al_2O_3 and 0.6BST may also create a space charge and thus influence the conductivity. The experimental conductivity data reported in this paper on the LATP–Al_2O_3 and LATP–0.6BST systems can be adequately explained using the blocking and space charge effects. Fig. 12 schematically shows the contributions of the two effects in the LATP–Al_2O_3 and LATP–0.6BST systems. In both cases, the blocking effect is more dominant than the space charge effect, leading to a peak in the conductivity around 27 °C for the 10 vol% of dopant concentration. Above 27 °C, the existence of the space charge is destroyed because of the thermal energy. The ions may be dissociated from the space charge region due to increased thermal energy ($kT > 0.026$ eV) and diffuse away from the interface at temperatures > 27 °C.

Fig. 12 also illustrates the difficulty in analyzing and interpreting conductivity data of heterogeneous solids. If the two effects are not considered independently, one may conclude that the space charge effect is non-existent in LATP–Al_2O_3 and LATP–0.6BST composites. The two effects coexist and only the temperature dependence study in the vicinity of the space charge

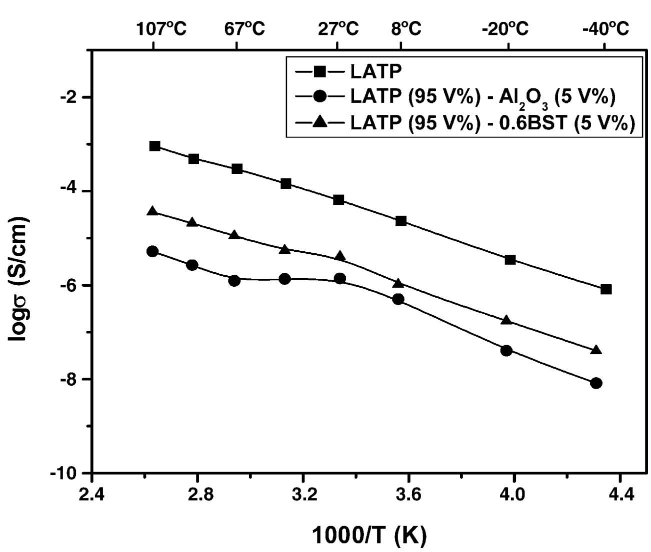

Fig. 10. Arrhenius plots of LATP–Al_2O_3 (5 vol%) and LATP–0.6BST (5 vol%) composites.

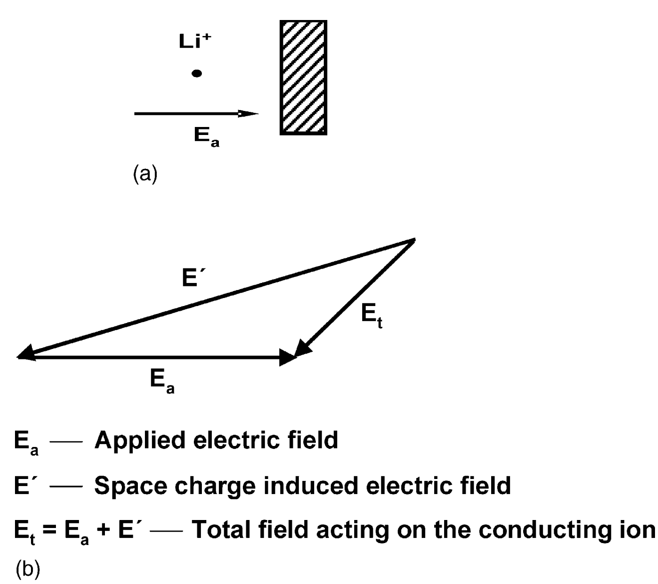

Fig. 11. Schematic presentation of (a) blocking effect and (b) space charge effect.

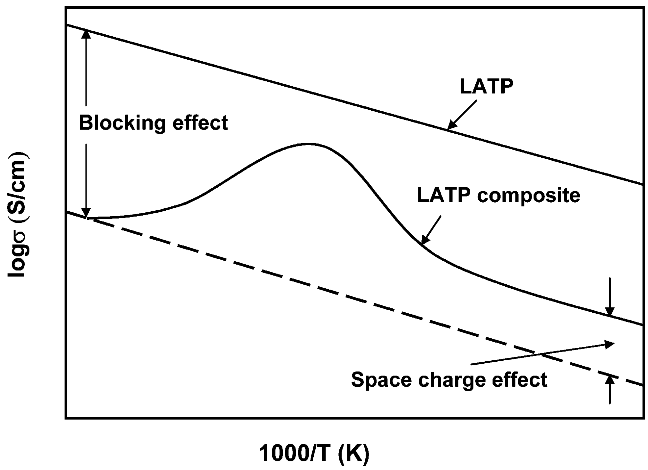

Fig. 12. Schematic presentation of blocking and space charge effect in LATP composites.

layer breakdown can distinguish their independent attributes. In the two systems, the space charge effect has a minor influence and is observed only at low temperatures.

In the LiI–Al_2O_3 system, the space charge effect is dominant in the 27–67 °C range (Fig. 2) and the net result is an increase in conductivity. The blocking effect also exists in LiI–Al_2O_3, but may be delineated by conductivity measurements at higher temperatures.

4. Summary and conclusions

1. The ionic conductivity of LiI and LATP ceramic were influenced by the addition of Al_2O_3 and 0.6BST. The conductivity of LiI was enhanced by the addition of Al_2O_3, whereas the conductivity of LATP was decreased with the addition of Al_2O_3 and 0.6BST.
2. It was proposed that two primary mechanisms could account for the observed experimental data in the LiI–Al_2O_3, LATP–Al_2O_3 and LATP–0.6BST systems. The first mechanism originates from the blocking effect of the dopant phase, whereas the second mechanism results from the space charge effect. These two mechanisms coexist in heterogeneous solids and their magnitudes differ from system to system. For example, in LiI–Al_2O_3, the space charge effect is dominant, whereas in the LATP–Al_2O_3 and LATP–0.6BST systems, the blocking effect is pronounced.
3. In the LATP–Al_2O_3 and LATP–0.6BST systems it was determined that the 0.6BST led to composites with higher conductivities, suggesting that the space charge effect is enhanced. Such an enhancement can be explained by considering the dielectric constants of Al_2O_3 and 0.6BST. The higher dielectric constant of 0.6BST is expected to create a larger space charge effect at LATP–0.6BST interfaces and thus augment lithium ion transport.
4. The peak observed in 10 vol% of LATP–Al_2O_3 and LATP–0.6BST system resulted from the influence of the blocking and the space charge effects. Ideally, both space charge and blocking effects exist together. In these systems, the space charge effect was dominant up to 27 °C and hence there was an increase in conductivity. The blocking effect took over later and the space charge effect was diminished due to increased thermal energy. In non-ionized lattice (LATP), both the blocking and space charge effects were operative. The conductivity peak results from the counteracting influences of the two.

References

[1] J. Maier, J. Phys. Chem. Solids 46 (1985) 309.
[2] J.S. Thokchom, C. Chen, K.M. Abraham, B. Kumar, Solid State Ionics 176 (2005) 1887.
[3] B. Kumar, C. Chen, C. Varanasi, J.P. Fellner, J. Power Sources 140 (2005) 12.
[4] C.C. Liang, J. Electrochem. Soc. 120 (1973) 1289.
[5] J. Maier, Prog. Solid State Chem. 23 (1995) 171.
[6] J. Fu, Solid State Ionics 96 (1997) 195.
[7] J.S. Thokchom, B. Kumar, Solid State Ionics 177 (2006) 727.